Short-Lived Intermediates in Aspartate Aminotransferase Systems

George Czerlinski,* Richard Levin,#, and Tjalling Ypma#
Departments of *Biology and #Mathematics, Western Washington University, Bellingham, Washington 98225 USA

ABSTRACT The kinetics of the reaction of aspartate aminotransferase with *erythro*-β-hydroxy-aspartate, in which rapid mixing is followed (upon reaching a suitable stationary state) by a very fast temperature jump, is numerically simulated. Values for rate constants are used to the extent known, otherwise estimated. It is shown that reaction steps not resolvable by rapid mixing can be resolved by subsequent chemical relaxation. Since several absorption spectra of enzyme complexes overlap, use of a pH-indicator is investigated. When the pH-indicator is coupled to the protonic dissociation of free enzyme, the fast steps are easily detected in the chemical relaxation portion of the simulation. When the pH-indicator is coupled to the protonic dissociation of the (short-lived) quinoid intermediate, protonic dissociation is easily detectable in the stopped flow phase and in the chemical relaxation phase. Such transient protonic dissociation has not been detected experimentally, but is predicted by the simulation. When natural substrates are used, the magnitude of the rate constants makes it unlikely that transient proton dissociation can be detected by stopped flow alone, but a combination of stopped flow with very fast temperature perturbation allows detection of the transient proton through use of a suitable nonbinding pH-indicator. This is demonstrated by simulation for a specific case. Finally, an alternate mechanism is introduced and distinction of its kinetics from that of the original mechanism is demonstrated.

INTRODUCTION

How to access short-lived intermediates in reaction systems and evaluate their reaction kinetics using a combination of rapid flow and very fast chemical relaxation was first discussed in 1992 (Czerlinski, 1992). Rapid mixing was used to enrich selected intermediates, and *much* faster temperature jump perturbation was then applied to investigate the very rapid interconversions among intermediates. This principle was also applied to fast equilibrations in the reaction of calmodulin with calcium ions (Czerlinski, 1992a). One may question the utility of a method that combines rapid mixing with much faster chemical relaxation. Such utility depends upon the number of systems that require a combination of rapid mixing with much faster chemical relaxation for the kinetics to be resolved. Aspartate aminotransferase has been independently investigated by both rapid mixing (Harruff and Jenkins, 1976, 1978; Jenkins and Harruff, 1979) and temperature jump relaxation (Czerlinski and Malkewitz, 1964; Fasella and Hammes, 1967). Both methods led to useful results, but both revealed steps that were not observed using the alternate method. As Jenkins summarized (Jenkins, 1980), there is also a problem with the cross-reaction of substrate and product with the opposing forms of the enzyme. This problem can best be circumvented by mixing substrate with the interacting form of the enzyme and initiating chemical relaxation *before* any product has formed. Here we investigate by numerical simulation to what extent a proper combination of the two methods will result in more information than using only a single one of the methods.

Aspartate aminotransferase is one of many enzymes using pyridoxal-5′-phosphate as tightly bound cofactor. This enzyme catalyzes the transamination of L-aspartate and L-glutamate to the respective 2-ketoacids. A key step in the pathway for almost all pyridoxal-5′-phosphate-dependent enzyme reactions is thought to involve the formation of a quinoid intermediate, Q (Metzler et al., 1954; Jenkins, 1961; Jenkins and Taylor, 1965). Evidence for the quinoid intermediate (or another species absorbing at 490 nm) in transamination reactions has been reported for the reaction of pig heart cytosolic aspartate aminotransferase with aspartic acid (Jenkins and Taylor, 1965) and for that of pig heart glutamic alanine transaminase with alanine and pyruvate (Jenkins, 1961). The quasi-substrate *erythro*-β-hydroxy-aspartate gives rise to an unusually long-lived quinoid intermediate with an absorption maximum at 492 nm (Jenkins and Taylor, 1965; Jenkins and Fonda, 1985).

The pyridoxal phosphate form of *Escherichia coli* aspartate aminotransferase catalyzes the conversion of L-cystein sulfinate to the pyridoximine phosphate form of the enzyme, bisulfite and pyruvate, with only the final step (of pyruvate formation) irreversible (Jenkins and Fonda, 1985). As this final step is also slow, intermediates appear including one with an absorption peak at 520 nm.

Details of the overall transamination reaction are shown in Fig. 1. This reaction may be abbreviated to the system of Eq. 1 shown in Fig. 2, which also introduces the eight rate constants for this reaction. Three intermediates are shown. In Fig. 2, A represents the amino acid (the substrate) and P the keto acid (the product); E is the enzyme form reacting properly with the amino acid, and F is the enzyme form reacting properly with the keto acid. The simulation of rapid mixing with chemical relaxation is first studied on the

Received for publication 20 September 1996 and in final form 22 November 1996.

Address reprint requests to Dr. George Czerlinski, P. O. Box 28521, Bellingham, WA 98228. Tel.: 360-671-6799; Fax: 360-671-6982; e-mail: ghc@henson.cc.wwu.edu.

0006-3495/97/03/1135/08 $2.00

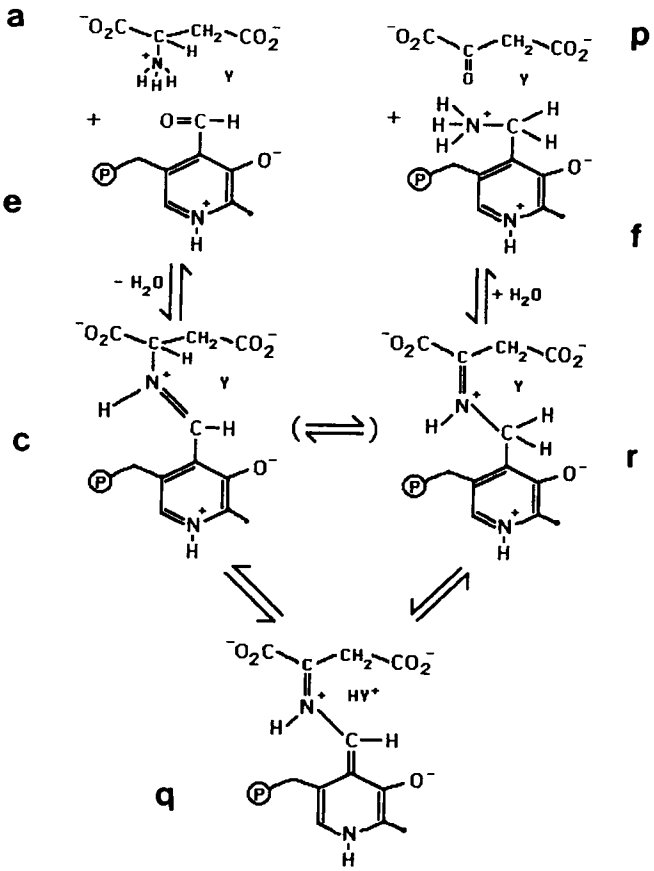

FIGURE 1 Reaction steps for the reaction of aminotransferase with aspartate showing the changes of structural details in the active site of the enzyme. The lower case letters around the periphery denote the concentration symbols used in the differential equations and in Figs. 3–10.

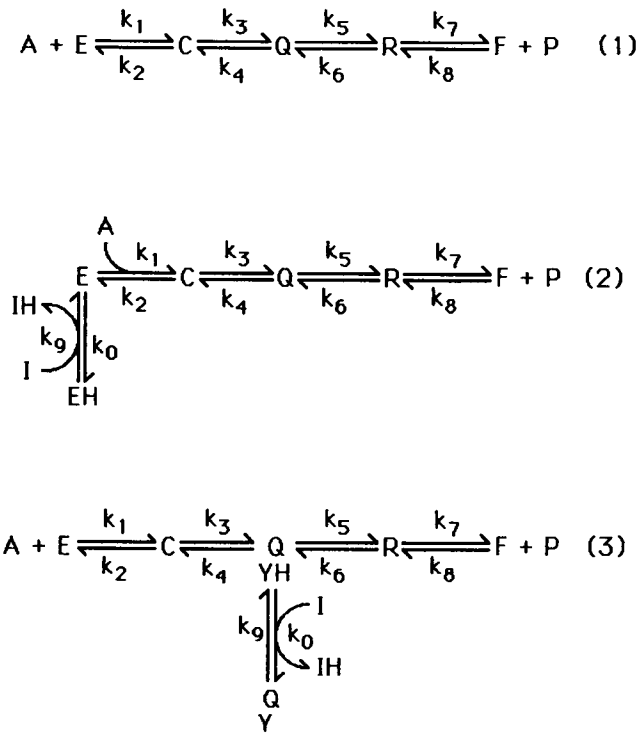

FIGURE 2 Symbolic equations of the reactions investigated. The concentration symbols used in Fig. 1 (*lower case letters*) become reactant symbols in Fig. 2 (as *upper case letters*). Consequently, Eq. 1 is the abbreviated version of the reaction in Fig. 1. Eq. 2 shows coupling of a pH-indicator to the proton dissociation of the enzyme. Eq. 3 shows coupling of a pH-indicator to a transiently existing *YH* on the enzyme (at *Q*).

reaction shown in Eq. 1 with the rate constant values for β-hydroxy-aspartate; this is *system 1*. Next, a pH-indicator is coupled to the protonic association involving *E*, Eq. 2 in Fig. 2, and the kinetics are simulated to elucidate transmission of the chemical relaxation of individual steps to the pH indicator: *system 2*. Next, a pH indicator is coupled to the protonic dissociation of *Q* (the *YH*-portion as shown in Eq. 3 of Fig. 2), and the appearance of the changes upon the indicator concentration are simulated: *system 3*. *System 4* is the same as system 3 except that the values of the rate constants are similar to those of the natural substrates instead of those for β-hydroxy-aspartate used in systems 1–3. Consequently, the high time resolution of the mixing apparatus becomes important.

We first establish the location of the slowest step(s) in three reactions of aspartate aminotransferase. Using estimates for the rate constants involved in these steps, we identify favorable conditions for the accumulation of short-lived intermediates. At the appropriate time in the course of the reaction we introduce a perturbation to initiate chemical relaxation. In practice, chemical relaxation is initiated by very fast temperature jumps produced by infrared laser pulses of proper duration, power, and geometry (Czerlinski, 1992). For numerical simulation, the results of a fast temperature jump are simulated by an instantaneous increase (by 30%) in the value of a suitable rate constant.

METHODS

Fig. 1 shows the general reaction scheme for the reaction of aspartate aminotransferase with substrate (or quasi-substrate), with one step placed in parentheses (reversed in the last section to evaluate an alternative mechanism). The step in parentheses is here specifically excluded, as structural reorientation is expected to be facilitated by the quinoid intermediate. This reaction scheme is abbreviated in Eq. 1 (see Fig. 2).

To establish values for the rate constants and initial values for the concentrations, specific reaction systems need to be discussed. "Natural systems" are those involving the natural substrates, aspartic acid and glutamic acid. One such system was investigated kinetically (Fasella and Hammes, 1967). They were only able to establish clearly one interconversion among intermediates, which they describe as the slowest one. Although they specifically use an "unlimited number" of intermediates, the one established is certainly very characteristic and is possibly the most important step in the reaction sequence. In terms of our reaction sequence it is temporarily assigned to the conversion of *Q* to *R*, see Eq. 1 and below. Fasella and Hammes (1967) determined $k' = 530/s$, and $k'' = 1130/s$ for the conversion of aspartate to oxalacetate (pH 8, pyrophosphate/HCl; their slowest step). They did not define the location of the rate constants in the reaction sequence. The values may belong to k_5 and k_6. The overall equilibrium constant of this half-reaction (at low enzyme concentration, 0.1 M pyrophosphate buffer, pH 8, 25°C) is (Jenkins and Taylor, 1965)

$$K'_{\text{half}} = \frac{[\text{oxalacetate}][\text{amino-enzyme}]}{[\text{aspartate}][\text{aldimine-enzyme}]} = 0.01 \qquad (4)$$

Thus, at comparatively low concentration of the aldimine-form of the enzyme with no oxalacetate initially present (most of the experiments reported), mixing experiments may be conducted up to the generation of R without interference by product P. Chemical relaxation could then be used to investigate the kinetics of the earlier reaction steps.

The presented overall reaction, Eq. 1, applies also to the system of converting glutamate to 2-ketoglutarate. Fasella and Hammes (1967) determined for this reaction $k' = 2940/s$, and $k'' = 1170/s$ (pH 8, pyrophosphate/HCl; their slowest step). They did not define the location of the rate constants in the reaction sequence. The values may belong to k_5 and k_6. The overall equilibrium constant of this half-reaction (at low enzyme concentration, 0.05 M pyrophosphate/HCl, pH 7.9) is (Jenkins and D'Ari, 1966)

$$K''_{\text{half}} = \frac{[\text{ketoglutarate}][\text{amino-enzyme}]}{[\text{glutamate}][\text{aldimine-enzyme}]} = 0.047 \quad (5)$$

Thus, at comparatively low concentration of the aldimine-form of the enzyme with no oxalacetate initially present (most of the experiments reported), one could proceed with mixing to produce Q and then investigate intermediate steps by chemical relaxation, as was described for the substrate aspartate.

At low enzyme concentration and with aspartate as first and glutamate as second substrate present one may also define the ratio $K'_{\text{half}}/K''_{\text{half}} = K_{\text{total}}$, given by

$$K_{\text{total}} = \frac{[\text{oxalacetate}][\text{glutamate}]}{[\text{aspartate}][\text{ketoglutarate}]} = 0.21 \quad (6)$$

More revealing in reference to intermediates is the half-reaction of *erythro*-β-hydroxyaspartate with the aldimine-form of the enzyme. Equation 1 still applies. Jenkins and Fonda (1985) determined $k_3 = 850/s$, $k_4 = 90/s$, $k_5 = 1.9/s$, and $k_6 = 2.9/s$ (pH 8, pyrophosphate/pyrophosphoric acid), using stopped flow instrumentation. The dissociation constant $k_2/k_1 = 0.1$ mM is estimated from Table 1 of Jenkins and Harruff (1985) for zero acetate concentration. The overall equilibrium constant of this half-reaction (at low enzyme concentration, 0.02 M sodium tetraborate, pH 9.2, 25°C) is estimated from Jenkins (1964)

$$K_{\text{half}} = \frac{[\text{OH-oxalacetate}][\text{amino-enzyme}]}{[\text{OH-aspartate}][\text{aldimine-enzyme}]} = 0.1 \quad (7)$$

System 1 uses the rate constants of Jenkins and Fonda (1985) together with estimates for the (diffusion-limited) bimolecular rate constants. Specifically, the values of the rate constants of column 2 of Table 1 apply. With these constants given, one may write the differential equations for system 1. Concentration symbols are defined in Fig. 1 next to the chemical formulas, and rate constants are defined in Fig. 2 with the one-letter symbols corresponding to the concentration symbols in Fig. 1. The set of differential equations is the same for all the above reaction systems, namely Eqs. 8–12 in Table 2. Equations 13 and 14 are given by the law of mass action and stoichiometry. Values for the *initial* concentrations after dilution from mixing (denoted by italic letters) are given in Table 1.

Equations 8–14 form a stiff system of differential equations, which was solved numerically by the Matlab routine ode23s (Shampine and Reichelt, 1997). The routine ode23s is a Matlab implementation (Matlab 4.2c, 1994) of an extremely stable variable-steplength second order modified Rosenbrock method (Hairer and Wanner, 1990). The results were plotted using the Matlab graphing facilities, with time shown on a logarithmic scale.

So far we have considered the transfer reaction without any auxiliary agents for detection. However, two proton dissociation reactions may be considered. These proton dissociations may then be coupled to suitable pH indicators for further detection of reaction kinetics.

In system 2A no substrate is present. The proton dissociation takes place sufficiently close to the active site that the protonated form interferes with substrate binding. This is denoted by

$$H + E \underset{k'_0}{\overset{k'_9}{\rightleftharpoons}} EH \quad (15)$$

This reaction can easily be investigated in the *absence* of any substrate. The pK_a (with $K_a = k'_0/k'_9$) in absence of interacting anions was determined as 5.73 (Jenkins, 1980), that is $pK(E, H) = p\{e\ h/(eh)\} = 5.73$, where (eh) is the concentration of component EH. Similarly, one may consider a nonbinding pH-indicator,

$$I + E \underset{k''_0}{\overset{k''_9}{\rightleftharpoons}} IH \quad (16)$$

with $K'_a = k''_0/k''_9$ or $pK'_a = pK(I, H) = p\{i\ h/(ih)\}$, where (ih) is the concentration of component IH. A nonbinding pH-indicator with $pK_a' \sim 5.73$ would be best for determining the kinetics (in a system of minimal pH-buffering). The proton transfer reaction between indicator I and enzyme E is then described by (omitting charges)

$$IH + E \underset{k_0}{\overset{k_9}{\rightleftharpoons}} EH + I \quad (17)$$

TABLE 1 Values for rate constants and initial concentrations

Parameters	System 1	System 2	System 3	System 4
k_1, $(sM)^{-1}$	$4.4 \cdot 10^8$	$4.4 \cdot 10^8$	$4.4 \cdot 10^8$	$4.4 \cdot 10^8$
k_2, s^{-1}	$4.4 \cdot 10^4$	$4.4 \cdot 10^4$	$4.4 \cdot 10^4$	$4.4 \cdot 10^4$
k_3, s^{-1}	850	850	850	$2.2 \cdot 10^4$
k_4, s^{-1}	90	90	90	$1.1 \cdot 10^4$
k_5, s^{-1}	1.9	1.9	1.9	2000
k_6, s^{-1}	2.9	2.9	2.9	250
k_7, s^{-1}	0.2	0.2	0.2	50
k_8, $(sM)^{-1}$	$1.2 \cdot 10^5$	$1.2 \cdot 10^5$	$1.2 \cdot 10^5$	$8 \cdot 10^8$
k_9, $(sM)^{-1}$		$5 \cdot 10^9$	$5 \cdot 10^9$	$5 \cdot 10^9$
k_0, $(sM)^{-1}$		$5 \cdot 10^9$	$5 \cdot 10^9$	$5 \cdot 10^9$
a, M	0.0004	0.0004	0.0004	0.0004
e, M	0.0001	0.0001	0.0001	0.0001
(eh), M	0	0.0001	0	0
j, M	0	0.00001	0.00001	0.00001
(ih), M	0	0.00001	0.00001	0.00001
$(q-H)$, M			0	0
(other), M	0	0	0	0

TABLE 2 Sets of differential equations

System	Equations	Equation No.
1	$da = (-k_1ae + k_2c)dt$	(8)
	$dc = (k_1ae - k_2c - k_3c + k_4q)dt$	(9)
	$dq = (k_3c - k_4q - k_5q + k_6r)dt$	(10)
	$dr = (k_5q - k_6r - k_7r + k_8fp)dt$	(11)
	$dp = (k_7r - k_8fp)dt$	(12)
	$de = da$	(13)
	$df = dp$	(14)
2	Eqs. 8 to 12 and 14 plus	
	$di = (k_9e(ih) - k_0i(eh))dt$	(21)
	$d(eh) = di = -d(ih)$	(22)
	$de = da - di$	(23)
3	Eqs. 8, 9, 11, 12, 13, 14 plus	
	$dq = (k_3c - k_4q - k_0iq + k_9(ih)q(-H) - k_5q + k_6r)dt$	(26)
	$di = (-k_0iq + k_9(ih)q(-H))dt$	(27)
	$d(ih) = dq(-H) = -di$	(28)

Without substrate present, the applicable differential equation is

$$di = (k_9 e(ih) - k_0 i(eh))dt \quad (18)$$

and the law of mass action and stoichiometry requires:

$$di = d(eh) = -d(ih) = -de \quad (19)$$

Chemical relaxation of this simplified system results in a single exponential term with the reciprocal relaxation time given by (Czerlinski, 1966)

$$k_9\{e + (ih)\} + k_0\{i + (eh)\}. \quad (20)$$

The two rate constants are determined from the concentration dependence of the reciprocal relaxation time.

In system 2B, substrate is present. When substrate is added to the system of free enzyme and pH indicator, one arrives at the mechanism of Eq. 2 of Fig. 2. From the previous system of differential equations we use Eqs. 8–12 and 14. We need to add Eq. 21 and Eqs. 22 and 23. The last two are based on the law of mass action and stoichiometry. The values of the rate constants are given in Table 1. The *initial* concentrations of species are determined for pH 5.73 (other pH-values may be chosen subsequently). These initial values are also shown in Table 1.

If the proton transfer reaction is fast enough (most likely it is diffusion limited), one may use this reaction step in the overall reaction of the enzyme with substrate to determine the kinetics of the binding of E with A, and possibly subsequent steps. If the pK_a values of the proton dissociation of enzyme and pH-indicator are matched, then forward and backward rate constants are the same, $k_9 = k_0$. One may estimate from the diffusion limit for small molecules $k_9 = 5 \times 10^9$/(s.M); this would be determined experimentally as described for system 2A. These diffusion-limited rate constants are then large enough to allow the detection of the concentration changes due to coupled-in slower steps in the overall reaction. The corresponding differential equations were also solved using the Matlab routine ode23s previously described.

System 3

The other proton dissociation reaction is connected with Q, or more precisely with the part of Q that holds a proton temporarily, namely Y (see Fig. 1):

$$H + Y \underset{k_0'}{\overset{k_9'}{\rightleftharpoons}} YH \quad (24)$$

As YH has only a transient life, its pK_a has never been determined. It is estimated at ~6. But as its transient life exists from pH 6 all the way up to pH 9, any (nonbinding) pH-indicator with pK in this range may be used. One might prefer to use two (or even more) such pH-indicators to cover the full pH-range effectively (in a system of minimal pH-buffering). If a sufficiently wide pH-range is accessible experimentally, one may enrich the concentration of Q by mixing and then initiate a temperature jump, observing the results from the pH-jump. The observed fast amplitude should pass through an extremum at the pK_H (Czerlinski, 1966). The following equation applies for proton transfer (omitting charges):

$$IH + Y \underset{k_0}{\overset{k_9}{\rightleftharpoons}} YH + I \quad (25)$$

One may use several pH-indicators, observing first when pH = pK_a of the indicator used (where the amplitude attains an extremum), then when pH > pK_a and finally when pH < pK_a (with the difference preferably not exceeding 1.0). One may use the same diffusion limited values for the rate constants of the proton transfer as described for system 2B. Incorporating Eq. 25 into Eq. 1 gives Eq. 3 (see Fig. 2). This reaction shows that the compound Q-Y is in a side branch of the reaction path. However, protonation from internal or external buffers takes place easily. This buffer capacity should be low enough that the change in indicator concentration is not buffer-suppressed below the detection limit. For purposes of this simulation, no buffering is assumed. The differential equations are the same as those given for system 1 except for the one involving Q, which is replaced by Eq. 26 (see Table 2) where $q(-H)$ is the concentration of component Q without the proton. Furthermore, Eq. 27 has to be added to account for the presence of the pH indicator, and Eq. 28 follows from the law of mass action and stoichiometry. In addition, Eqs. 13 and 14 have to be included. Appropriate values for the rate constants and *initial* concentrations are listed in Table 1. The differential equations are also solved using the Matlab routine ode23s previously described.

System 4

The intermediate Q is easily detected with the artificial substrate *erythro*-β-hydroxy-aspartate through the absorption band of Q or the pH-indicator, assuming very fast proton transfer. If this proton transfer is fast, it should also appear in reactions with the *natural* substrates aspartate and glutamate. These reactions were discussed earlier, when some characteristic constants were given. Unfortunately, those constants cannot be used for this simulation, as component Q would have to be present in significant concentration at equilibrium. Values for the rate constants used are those from column 5 of Table 1 (with aspartate as substrate and with indicator I present for coupling to YH). These values are limited for bimolecular steps by diffusion and for monomolecular steps by the rate constants (range) determined by Fasella and Hammes (1967). The *initial* concentrations for the numerical simulation are the same as those indicated for the artificial substrate (see column 5 of Table 1). The differential equations, identical to those for system 3, are again solved using the Matlab routine ode23s

RESULTS and DISCUSSION

Results of the simulations are shown in Figs. 3 through 10, the first six of which refer to *erythro*-β-hydroxy-aspartate as substrate. Fig. 3 refers to system 1 and clearly shows the separation of the reaction steps along the logarithmic time axis. As the time resolution of the planned mixing instru-

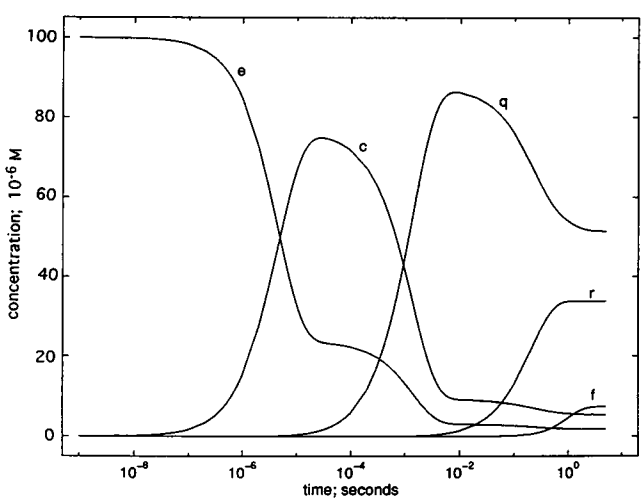

FIGURE 3 Simulation of "instantly" mixing equal concentrations of *erythro*-β-hydroxy-aspartate with the keto-form of aminotransferase (100 [um]M) and observing the concentrations of intermediates and the two forms of the enzyme. Concentrations e refer to free keto-form of the enzyme, c to the first intermediate, q to the quinoid intermediate, r to the last intermediate and f to the free amino-form of the enzyme. Applicable rate constants are given in the text.

ment is at best limited to 0.0001 s, the kinetic changes of concentration c cannot be followed with a flow apparatus. Fig. 4 reveals the events after a nanosecond temperature jump initiated 0.01 s after mixing (Fig. 3) when q is near its maximum value, simulated by increasing k_1 by 30%. Only one rate constant is changed upon the temperature rise, to demonstrate the propagation of this change through the reaction system. The time scale is reset (to zero) to allow visibility of the very rapid relaxation processes. Fig. 4 (*top*) shows the change in q (*dotted curve*) relative to the curve with k_1 unchanged (*solid curve*). Concentration c in Fig. 4 (*bottom*) shows a transient positive change due to the temperature change. At the new equilibrium (reached at 5 s) only e remains changed significantly from the prior equilibrium. The results in Fig. 4 (*bottom*) show that the fast changes in the concentrations c and e are detectable by chemical relaxation.

Fig. 5 shows the concentration of all components (including i, the concentration of the indicator) as they change with time during the simulation of the "instant" mixing experiment (meaning, mixing is considered complete within nanoseconds) with the indicator coupled to the free unprotonated enzyme, e (system 2B, simply system 2). The concentration of the indicator is relatively small to reduce the effect of the indicator concentration on the overall reaction (it responds easily to changes, not buffering them). However, the indicator is expected to have a much larger molar extinction coefficient than any of the enzyme intermediates, facilitating the detection by indicator (especially if peak extinction of i is >520 nm). Interestingly, all reaction steps are visible in the changes of the indicator concentration alone (except the last one, producing p). This concentration i changes from 10 μM to ~4 μM with the appearance of c, then

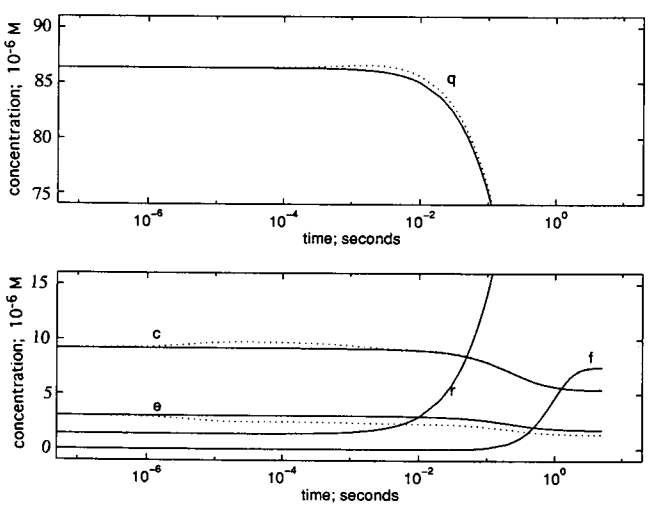

FIGURE 4 A temperature jump is initiated 0.01 s after mixing (see Fig. 3). Only the time following the "instant" temperature jump is shown. Full lines refer to zero perturbation (k_1 remains unchanged). Dotted lines refer to those corresponding to perturbation (k_1 increased by 30% as consequence of the temperature jump). Fig. 4 (*top*) only shows the changes of q; Fig. 4 (*bottom*) shows the changes of e and of c.

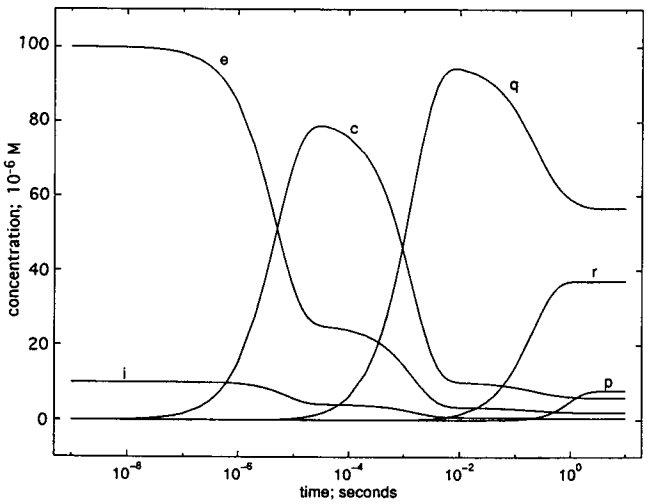

FIGURE 5 Simulation of "instantly" mixing 400 μM *erythro*-β-hydroxy-aspartate with 100 μM unprotonated keto-form of aminotransferase coupled by pH-indicator to 100 μM protonated keto-form and observing the concentration of the indicator, i, as well as those of components E, C, Q, R, and P. The whole reaction sequence is reflected in changes of the indicator concentration, although they become minuscule at the end.

decreases to ~0.74 μM with the appearance of q, and finally decreases to 0.45 μM. To observe these latter changes, a very high molar extinction coefficient of i relative to ik would be needed (or fluorescence detection). However, since these changes occur in the time range accessible by stopped flow, this is not a significant concern.

Fig. 6 reveals the events as indicated by i after a nanosecond temperature jump initiated 0.01 s after mixing when q is near its maximum value (Fig. 5). The two faster steps are clearly indicated in changes of the indicator concentration i, although the changes in c and q are not easily detected directly with the present choice of the time at which the

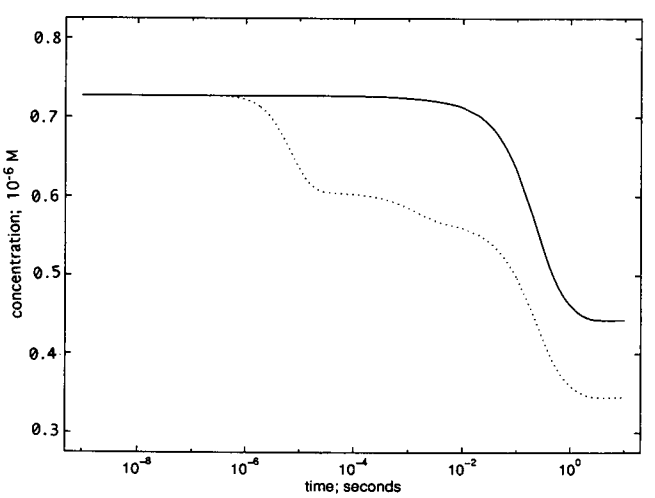

FIGURE 6 A temperature jump is initiated 0.01 s after mixing (see Fig. 5). Full lines refer to zero perturbation (k_1 remains unchanged). Dotted lines refer to those corresponding to perturbation (k_1 increased by 30%).

temperature jump is initiated (0.01 s) because of their overlapping extinction coefficients.

Fig. 7 shows the concentration of the indicator i changing with time during the simulation of the "instant" mixing experiment with the indicator coupled to the protonated quinoid form q (system 3). In contrast to Fig. 5, a decrease in e and increase in c are not visible, as these steps are faster than the appearance of q to which i is coupled. Only the appearance of q is clearly reflected in the stepwise decrease of i. Again, the concentration of the indicator is relatively small to reduce the effect of the indicator concentration on the overall reaction (no "buffering"). But the indicator is expected to have a much larger molar extinction coefficient than any of the enzyme intermediates, facilitating detection by the indicator.

Fig. 8 reveals the events detected by i after a nanosecond temperature jump initiated 5 s after mixing, when q is near its equilibrium value rather than at its maximum value (with only k_3 increased by 30%). Performing a temperature jump clearly shows increase and decrease of q in curve i (the only one shown). Again (as in Fig. 7), the faster changes in e and q are not detectable by way of i.

Fig. 9 shows the simulated mixing of free transaminase with the natural substrate aspartate and with a pH-indicator present for coupling to component Q (specifically portion YH: system 4). System 4 is identical to system 3 (with Figs. 7 and 8), differing only in most rate constants, which are much faster in system 4 (just as in the natural system). Events are thus compressed along the time axis compared to those in Fig. 7.

Figure 10 shows the effect of a temperature jump, executed 0.01 s after mixing when equilibrium has essentially been reached. Only a change in the indicator concentration is shown. The dotted curve refers to an increase of only one rate constant, k_3 (by 30%). The total change in Fig. 9 is only

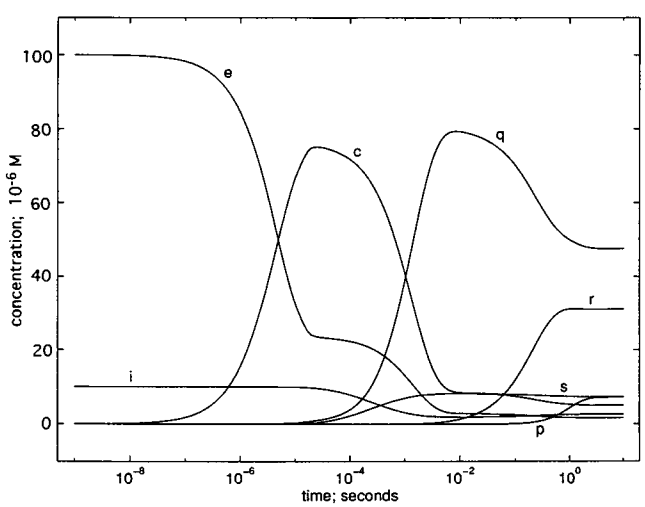

FIGURE 7 Simulation of "instantly" mixing 400 μM *erythro*-β-hydroxy-aspartate with 100 μM keto-form of aminotransferase and observing the concentrations of intermediates and the two forms of the enzyme from instant of mixing to equilibration.

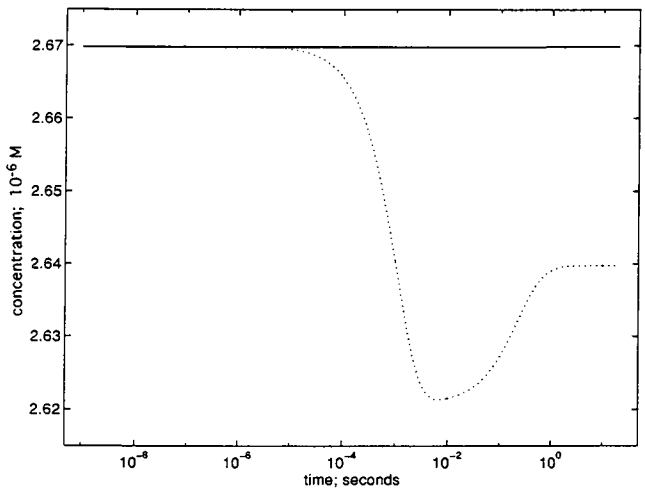

FIGURE 8 A temperature jump is initiated 5 s after mixing (see Fig. 7) showing only the concentration of the (unprotonated) pH-indicator. Full lines refer to zero perturbation (k_3 remains unchanged). Dotted lines refer to those upon perturbation by temperature jump (only k_3 increased by 30%).

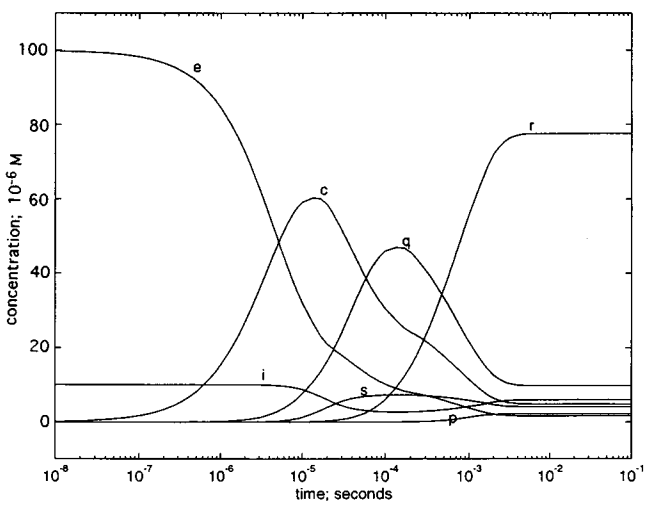

FIGURE 9 Simulation of "instantly" mixing 400 μM aspartate with 100 μM keto-form of aminotransferase and observing the concentrations of intermediates and the two forms of the enzyme from instant of mixing to equilibration.

0.15 μM on a background of ~6 μM (thus 2.5%). Only use of a fluorescent pH-indicator would allow the detection of such a small change. This change may actually occur in a faster time range than shown.

While some of the events in Fig. 7 can be (and have been) resolved by ordinary flow experiments, such experiments are essentially useless for Fig. 9, as most flow instruments have time resolutions only down to ~1 ms. Although ordinary T-jump experiments can be (and have been) conducted, the ordinary equilibration time is too long, leading to cross-reactions of P with E and A with F (compare Fig. 2). Only fast mixing with T-jump before long equilibration (such as at 0.01 s after mixing) can provide reliable results. Further-

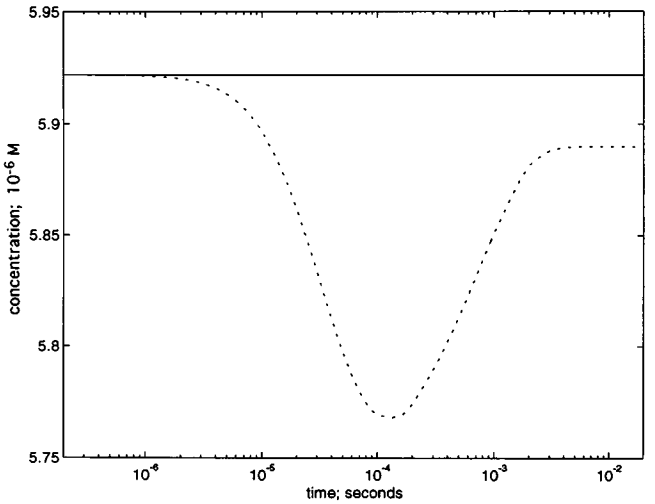

FIGURE 10 A temperature jump is initiated 0.01 second after mixing (see Fig. 9) showing only the concentration of the (unprotonated) pH-indicator. Full lines refer to zero perturbation (k_3 remains unchanged). Dotted lines refer to those upon perturbation by temperature jump (only k_3 increased by 30%).

more, referring to Fig. 5, by using a very fast mixing apparatus one could initiate a T-jump near the maximum of c and observe the changes to this maximum by chemical relaxation of the pH-indicator alone. One would see the first inflection in Fig. 6 (*dotted line*), only accessible by T-jump experiments. Similarly, if system 2 would be changed to the equivalent of system 4 (that is, only values of rate constants are increased) and if the T-jump would take place near the maximum of q, all faster steps would be seen by changes in the pH-indicator concentration. In other words, only a combination of the temperature jump method with rapid mixing allows us to reveal complete mechanistic details.

The basic assumption for all systems was that the reaction times of the various steps in the transfer reaction increase from left to right. This has been proven partially only for *erythro*-β-hydroxy-aspartate. If this assumption is not fulfilled for the natural substrates, one may initiate the reaction by mixing the components shown on the right side (namely F and P, Eq. 1). As the overall equilibrium reveals preference for components on the left side (namely E and A), this alternate mixing procedure may have advantages for the investigation of all reaction systems. But the danger that A forms an abortive complex with F is then more likely during the course of the reaction, requiring a careful timing of the temperature jump.

DISCUSSION: ALTERNATE MECHANISM

In Fig. 1, one reaction step was placed in parentheses. Let us now focus on this step and add rate constants:

$$C \underset{k_{21}}{\overset{k_{12}}{\rightleftharpoons}} R \tag{26}$$

With these interconversion rate constants, insignificance of the step in parentheses is quantitatively expressed by

$$k_{12}, k_{21} \ll k_3, k_4, k_5, k_6 \tag{27}$$

The opposing relation is given by

$$k_{12}, k_{21} \gg k_3, k_4, k_5, k_6 \tag{28}$$

Let us now consider relation 28 as basis for an "alternate mechanism." If at the same time

$$k_{12}, k_{21} \ll k_1(a + e), k_2, k_8(p + f), k_7 \tag{29}$$

one may establish a point in time where equilibration of the three fastest steps has been reached, while essentially no Q has been formed as yet. Chemical relaxation (initiated by temperature jump) at that point would result in a third relaxation time (see Czerlinski, 1966),

$$t_3^{-1} = k_{12}(a + e)/(a + e + k_2/k_1) + k_{21}(p + f)/(p + f + k_7/k_8) \tag{30}$$

This relaxation time could *not* be seen by observing only Q or fast reactions coupled to Q (such as pH-indicator systems).

Relation 28 states nothing about the relation between the pairs of rate constants on the right side. If these relations are pronounced, one may distinguish

$$k_3, k_4 \ll k_5, k_6 \tag{31}$$

from

$$k_3, k_4 \gg k_5, k_6 \tag{32}$$

Let us consider relation 31 first. Components C and R are equilibrated before the reaction between R and Q is initiated. When their equilibration is reached, the whole system is in equilibrium. Thus, k_3 and k_4 never enter into any kinetic process. Observation of Q (directly or through an indicator) would only reveal the kinetic process between Q and C. The reactions determined by the rate constants in relation 29 would couple into k_6 as equilibrium relation (pre-equilibration). It would not matter whether the mixing is started from the side shown in the above presentation ($a + e$), or from the other side ($p + f$). Only one of the two steps discernible in Fig. 8 (or even Fig. 10) would be visible. This is the striking difference between the two alternative mechanisms. In addition, r and p in Fig. 7 would not rise above zero after q and s do so, but before.

Unfortunately, these differences can not be extracted from either Fig. 5 or Fig. 6, as far as the indicator is concerned. In Fig. 5, only four levels in the indicator concentration (i) are discernible. There should be one each for e, c, q, r, and p, thus five. But the increase in p is very small and simply not discernible on the scale presented for i. This has also experimental implications insofar as ordinary indicators would not allow visibility of five steps. Properly chosen fluorescent indicators could. Even if these differences could be extracted from the changes in indicator concentration, the assignment of time changes to concen-

tration changes of specific components could not. Detection by way of Q becomes a necessity.

Now let us consider relation 32. Again, components C and R are equilibrated before the reaction between C and Q is "turned on." When their equilibration is reached, the whole system is in equilibrium; thus, k_5 and k_6 never enter into a kinetic process. Observation of Q (directly or through an indicator) would only reveal the kinetic process between Q and R. The reactions contained in relation 29 would couple into k_3 as equilibrium relation (pre-equilibration). It would not matter whether the mixing is started from the side shown in the above presentation ($a + e$), or from the other side ($p + f$). Again, only one of the two steps discernible in Fig. 8 (or even Fig. 10) would be visible. This is the striking difference between the two mechanisms (namely Eq. 27 versus Eq. 28). In addition, r and p in Fig. 7 would not rise above zero after q and s, but before.

It should be pointed out that observation by way of Q does not allow one to distinguish between the alternatives of Eqs. 31 and 32. We would not know without other information how the equilibrium factor with k_3 (or k_6) is actually structured. Only carefully conducted flow experiments from both sides with chemical relaxation at various points along the mixing time scale with and without the aid of (nonbinding) pH-indicators could reveal all the kinetic steps quantitatively.

However, this quantitative determination becomes more difficult if any of the relations "$\gg$" and "$\ll$" degenerate to "$>$" and "$<$." The more this degeneration is expressed, the more difficult it becomes to determine actual rate constants with any precision from experimental data. This is a general problem of chemical kinetics.

REFERENCES

Czerlinski, G. 1966. Chemical Relaxation. Marcel Dekker, New York.

Czerlinski, G. 1992. On the problem of kinetically hidden reaction steps. *J. Theor. Biol.* 154:119–126.

Czerlinski, G. 1992a. Resolving the fast equilibrations between calmodulin and calcium ions. *Physiol. Chem. & Physics.* 24:213–226.

Czerlinski, G., and J. Malkewitz. 1964. Chemical relaxation spectrum of glutamic aspartic aminotransferase/*erythro*-β-hydroxyaspartate. *Biochemistry.* 4:1127–1137.

Fasella, P., and G. G. Hammes. 1967. A temperature jump study of aspartate aminotransferase. A reinvestigation. *Biochemistry.* 6:1798–1804.

Hairer, E., and G. Wanner. 1990. Solving Ordinary Differential Equations II: Stiff and Differential-Algebraic Problems. Springer, Berlin.

Harruff, R. C., and W. T. Jenkins. 1976. The effect of halides on the equilibrium and reactivity of aspartate aminotransferase. *Arch. Biochem. Biophys.* 177:394–401.

Harruff, R. C., and W. T. Jenkins. 1978. The mechanism of anion inhibition of pork heart aspartate aminotransferase. *Arch. Biochem. Biophys.* 188:37–46.

Jenkins, W. T. 1961. Vitamin B-6 coenzymes and mechanism of transamination. *Fed. Proc. Am. Soc. Exp. Biol.* 20:978–981.

Jenkins, W. T. 1964. Glutamic-aspartic transaminase. VII. Equilibrium kinetics with *erythro*-β-hydroxyaspartic acid. *J. Biol. Chem.* 239: 1742–1747.

Jenkins, W. T. 1980. The specific anion effect on the chromophoric proton dissociation of heart aspartate aminotransferase. *Arch. Biochem. Biophys.* 205:579–586.

Jenkins, W. T. 1986. Kinetic and equilibria studies with pyridoxal phosphate enzymes. *In* Pyridoxal Phosphate: Chemical, Biochemical, and Medical Aspects, Part A, Vol. 1A. Dolphin, editor. John Wiley & Sons, New York.

Jenkins, W. T., and L. D'Ari. 1966. Glutamic-aspartic transaminase. IX. Equilibria with glutamate and ketoglutarate. *J. Biol. Chem.* 241: 2845–2854.

Jenkins, W. T., and M. L. Fonda. 1985. Kinetics, equilibria, and affinity for coenzymes and substrates. *In* Transaminases, P. Christen and D. E. Metzler, editors. Wiley-Interscience, New York, 233.

Jenkins, W. T., and R. C. Harruff. 1979. Solvent and substrate deuterium isotope effects on a transamination reaction catalyzed by pig heart aspartate aminotransferase. *Arch. Biochem. Biophys.* 192:421–429.

Jenkins, W. T., and R. T. Taylor. 1965. Glutamic-aspartic transaminase. VIII. Equilibrium kinetics with aspartate. *J. Biol. Chem.* 240:2907–2913.

Matlab 4.2C. 1994. The MathWorks, Inc., 24 Prime Park Way, Nattick, MA.

Metzler, D. E., M. Ikawa, and E. E. Snell. 1954. A general mechanism for vitamin B6-catalyzed reactions. *J. Am. Chem. Soc.* 76:648–652.

Shampine, L. F., and M. W. Reichelt. 1997. The Matlab ODE Suite. *SIAM J. Sci. Computation* 18: (in press).